ACS APPLIED MATERIALS & INTERFACES

Research Article

www.acsami.org

Hydrothermal Synthesis and Characterization of Aluminum-Free Mn-β Zeolite: A Catalyst for Phenol Hydroxylation

Zhen He,*[,†] Juan Wu,[‡] Bingying Gao,[‡] and Hongyun He[‡]

[†]College of Chemistry and Chemical Engineering, Central South University, Changsha, Hunan 410083, P. R. China

[‡]Key Laboratory of Chemical Biology and Traditional Chinese Medicine Research, Ministry of Education, Hunan Normal University, Changsha, Hunan 410081, P. R. China

Supporting Information

ABSTRACT: Zeolite beta, especially heteroatomic zeolite beta, has been widely used in the industries of fine chemicals and petroleum refining because of its outstanding thermal stability, acid resistance, and unique 3-D open-frame structure. In this paper, aluminum-free Mn-β zeolite was hydrothermally synthesized in the SiO_2−MnO_2−$(TEA)_2O$−NaF−H_2O system. The effect of the chemical composition of the precursor mixture to the crystallization of the Al-free Mn-β zeolite was investigated. The synthesized Al-free Mn-β zeolite was characterized by inductively coupled plasma (ICP), XRD, thermogravimetric/differential thermal analysis (TG/DTA), N_2 adsorption−desorption, FT-IR, UV−vis, X-ray photoelectron spectroscopy (XPS), and scanning electron microscope (SEM). The results show that the synthesized zeolite has a structure of β zeolite with good crystallinity and Mn ions present in the framework of the zeolite. The synthesized Al-free Mn-β zeolite shows great catalytic activity toward the phenol hydroxylation reaction using H_2O_2 as the oxidant. Approximately 35% of phenol conversion and ∼98% of dihydroxybenzene selectivity can be obtained under the optimal conditions.

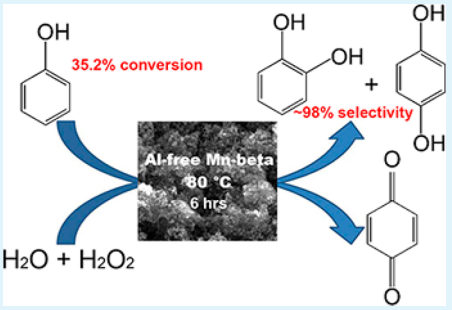

KEYWORDS: *beta zeolite, hydrothermal synthesis, Al-free, phenol hydroxylation, catalytic activity*

1. INTRODUCTION

Zeolite beta, as a three-dimensional large-pore zeolite, has attracted much attention due to its wide applications as a catalyst for oil refining, petrochemistry, organic synthesis of fine and specialty chemicals, and inorganic selective reduction of NO_x and also as an adsorbent for gas separation.[1−5] The catalytic activities of zeolite beta depend on the incorporation of aluminum or/and other metallic atoms (heteroatoms) into the framework of zeolite beta.[6] Zeolite beta with different architectures and acid site densities and strengths have been synthesized hydrothermally by using different structure-directing agents (SDAs) and by adding sources of heteroatoms into the synthesis precursors.[7] Heteroatomic zeolite beta (that is, the zeolite beta with a part of the framework aluminum or/and silicon ions being isomorphously substituted by other metal ions) is of particular interest because it shows enhanced activity, selectivity, and lifetime over its parent zeolite beta for certain reactions.[8] Ti-beta zeolite (Ti-β) exhibited selectivities for epoxides close to 100% in olefin epoxidation using *tert*-butyl hydroperoxide (TBHP) as the oxidant.[9] Corma and co-workers reported Sn-β as an efficient and stable heterogeneous chemoselective catalyst for Baeyer−Villiger (BV) oxidation of ketones to the reaction products with more than 98% lactones.[10] Following this work, they also reported that Sn-β showed high activity and selectivity for the cyclization of citronellal to isopulegol (cyclic carbonyl-ene reaction) and Meerwein−Ponndorf−Verley−Oppenauer (MPVO) redox reactions.[11−14]

Many manganese compounds have shown potent catalytic activities toward different reactions such as water oxidation,[15−18] oxygen reduction reaction (ORR),[17−19] styrene epoxidation,[20] and oxidation of phenol.[21] Therefore, many efforts have been dedicated to incorporating Mn ions into zeolitic materials, attempting to combine these two types of catalytic materials for synergistic catalytic activities. Meng et al. recently synthesized a manganese-containing MFI-type zeolite (Mn-ZSM-5) with remarkable activity in catalyzing both benzyl alcohol oxidation and toluene oxidation.[22] Raja et al. reported framework-substituted manganese aluminophosphate zeolite (MnAlPO-5) catalysts for the selective oxidation of cyclohexane in air.[23] Parida et al. demonstrated the amination of benzene to aniline with 100% selectivity by using mesoporous Mn-MCM-41 as the catalyst.[24] Framework-substituted manganese zeolite beta (Mn-β) has also been reported. Zhang et al. showed the hydrothermally synthesized Mn−Al-β as a carrier of the Pt catalyst for hydroisomerization of *n*-heptane.[25] Ogura et al. synthesized the Mn-containing Al-β through a solid-phase transformation of mesoporous Mn-MCM-41 and used it as a hydrocarbon reformer trap.[26] However, to the best of the

Received: October 15, 2014
Accepted: January 3, 2015
Published: January 3, 2015

DOI: 10.1021/am507134g
ACS Appl. Mater. Interfaces 2015, 7, 2424−2432

Table 1. Influence of Chemical Compositions in the Precursor Mixture on the Crystallization of Al-Free Mn-β Zeolite[a]

group	sample	molar ratios in precursor mixture (% mol) $n(SiO_2):n(MnO_2):n[(TEA)_2O]:n(H_2O):n(NaF)$	XRD results
Group I: Samples 1−7	1	60:0.1:18:450:10	amorphous phase(s)
	2	60:0.3:18:450:10	β
	3	60:0.5:18:450:10	β
	4	60:1.0:18:450:10	β
	5	60:2.5:18:450:10	β
	6	60:3.0:18:450:10	β
	7	60:3.2:18:450:10	amorphous phase(s)
Group II: Samples 8−13	8	60:1.0:10:450:10	amorphous phase(s)
	9	60:1.0:11:450:10	amorphous phase(s)
	10	60:1.0:12:450:10	β
	11	60:1.0:15:450:10	β
	12	60:1.0:16:450:10	β
	13	60:1.0:18:450:10	β
Group III: Samples 14−18	14	60:1.0:18:350:10	amorphous phase(s)
	15	60:1.0:18:450:10	β
	16	60:1.0:18:650:10	β
	17	60:1.0:18:750:10	β
	18	60:1.0:18:850:10	β+other phase(s)
Group IV: Samples 19−24	19	60:1.0:18:450:4	amorphous phase(s)
	20	60:1.0:18:450:6	β
	21	60:1.0:18:450:10	β
	22	60:1.0:18:450:12	β
	23	60:1.0:18:450:18	β
	24	60:1.0:18:450:20	β+other phase(s)

[a]This table consists of four groups of experiments (that is, samples 1-7, 8-13, 14-18, and 19-24, respectively) studying the concentrations of MnO_2, TEA_2O, H_2O, and NaF in the precursor mixture on the crystallization of Al-free Mn-β, respectively. Note that the results of sample nos. 4, 13, 15, and 21 are actually based on the same sample. It is repeatedly shown in Groups I−IV for the consistency of data and convenience of comparison.

authors' knowledge, all the reported Mn-β have Al^{3+} ions (strong acidic centers) in the frameworks, which limits their applications in some reactions involving H_2O_2 (e.g., phenol hydroxylation reaction using H_2O_2 as the oxidant), because the strong acidic centers (framework-Al sites) accelerate the decomposition of H_2O_2 and thus lower the conversion percentage of the reactants. Here, we present the hydrothermal synthesis of the highly crystalline Al-free framework-substituted Mn-β with a tunable Mn concentration in the range of 0−3.56 wt %. The synthesized Al-free Mn-β zeolites have shown great catalytic activity toward the phenol hydroxylation reaction using H_2O_2 as the oxidant. Under the optimized experimental conditions, ∼35% of phenol conversion and ∼98% of dihydroxybenzene selectivity in the products can be obtained.

2. EXPERIMENTAL SECTION

2.1. Synthesis of Al-Free Mn-β. The synthesis precursor mixtures with the molar compositions of SiO_2:MnO_2:$(TEA)_2O$:H_2O:NaF = 60:(0.3−3):(12−18):(450−750):(6−18) were used to synthesize Al-free Mn-β. These precursor mixtures were typically prepared in three steps. First, appropriate amounts of $MnSO_4 \cdot H_2O$ (≥99% purity, Tianjin Chemical Reagent Research Institute) and tetraethylammonium hydroxide solution (TEAOH, 21 wt % aqueous solution, Hunan Jianchang Petrochemical Co., Ltd.) were added into deionized water (DI water). The mixture was stirred for 2 h in an open container and turned to a brown colloidal solution, which was a uniform mixture of $MnO(OH)_2$ and TEAOH. Second, SiO_2 powder (99.9% purity, Shenyang Chemical Co., Ltd.) was slowly added into the colloidal solution under vigorous stirring and stirred for another 2 h. Third, an appropriate amount of NaF (analytical grade, Tianjin Chemical Reagent Research Institute) dissolved in DI water was added into the mixture. The mixture was further vigorously stirred for 2−3 h to form the precursor mixture used to synthesize Al-free Mn-β zeolites.

For the crystallization of Al-free Mn-β, the as-prepared precursor mixture was transferred into an autoclave with a Teflon lining and crystallized at 140 °C in an oven for 12 days. After the crystallization process, the product in the autoclave was separated from the solution by high-speed centrifugation and washed by DI water until the pH of the eluate approached 7. The washed product was desiccated at 100 °C for 4 h before further characterizations. The synthesized Al-free Mn-β samples used in catalyzing the phenol hydroxylation reaction were additionally calcined at 550 °C in air for 4 h in order to further remove the organic template.

2.2. Characterization of Al-Free Mn-β. The crystal structure of the Al-free Mn-β was analyzed by using a Y-2000 X-ray diffractometer with a Ni-filtered Cu Kα_1 radiation source (λ = 0.15406 nm) at 40 kV and 20 mA. The $\theta-2\theta$ scan was obtained in the range of 4° to 40° with a scan rate of 4°/min. The unit cell volume of the Al-free Mn-β was calculated by using the cell refinement software (integrated in the Y-2000 X-ray diffractometer system) based on the tetragonal crystal system.

The morphology of the synthesized Al-free Mn-β was studied by an FEI Nova NanoSEM 450 scanning electron microscope (SEM) at an accelerating voltage of 10 kV.

The adsorption and desorption isotherms were measured at −196 °C on a Micrometritics TriStar 3000 instrument at relative pressures (P/P_0) from 0.01 to 0.989 and from 0.989 to 0.01, respectively. Samples were degassed at 300 °C and 10^{-6} Torr for 6 h before each measurement to remove physically adsorbed species.

The FT-IR spectrum was taken from pressed pellets of a KBr diluted Al-free Mn-β sample on a Nicolet Avatar 370 FT-IR spectrometer in the range of 1400−400 cm^{-1}.

The UV−vis diffuse reflectance spectrum (UV−vis DRS) of the Al-free Mn-β was collected using a Hitachi U-3310 UV−vis spectrophotometer with a Φ150 mm integrating sphere accessory.

DOI: 10.1021/am507134g
ACS Appl. Mater. Interfaces 2015, 7, 2424−2432

The thermogravimetric/differential thermal analysis (TG/DTA) of the Al-free Mn-β sample was carried out on a NETZSCH-STA409PC thermal analyzer in the temperature range of 20−800 °C with a heating rate of 10 °C min^{-1} in air.

The manganese content in the synthesized Al-free Mn-β was measured by a PerkinElmer Optima 3300 DV inductively coupled plasma (ICP) elemental analyzer. The Al-free Mn-β sample (~0.1 g) was dissolved in ~2 mL of HF (40 wt % in H_2O). The formed solution was acidified with ~40 mL of 2.0 M HCl and heated in order to remove HF and then filtered. The filtrate was then diluted and tested by the ICP.

Surface analysis of the synthesized Al-free Mn-β was done on a Thermo Scientific ESCALAB 250Xi X-ray photoelectron spectrometer (XPS) using monochromatic Al Kα radiation energy (λ = 1486.6 eV).

2.3. Catalytic Activity of Al-Free Mn-β toward the Phenol Hydroxylation Reaction. The calcined Al-free Mn-β was used as a catalyst for the phenol hydroxylation reaction. For comparison, Al-β was also used as the catalyst for the phenol hydroxylation reaction under the same experimental conditions. H_2O_2 solution (30 wt %) (Tianjin Chemical Reagent Research Institute) and DI water were used as the oxidant and solvent of the reaction, respectively. The reaction was processed at 1 atm in a round-bottom flask equipped with a reflux condenser, a magnetic stirrer, and a temperature-controllable water bath. An amount of 2 g of phenol was added to ~33 mL of DI H_2O in the flask, followed by the addition of a calculated amount of the catalyst (mass ratios of catalyst/phenol = 1/15, 1/20, 1/25, and 1/30, respectively, in separated tests). After the mixture was heated to the desired temperature (60, 70, 80, and 90 °C, respectively, in different experiments), a calculated amount of H_2O_2 (30 wt %) was added into the mixture through a syringe (molar ratios of phenol/H_2O_2 = 1/1, 2/1, 3/1, and 4/1, respectively, in separated tests). The product was sampled by a syringe and filtered in order to remove the catalyst particles. The reactant mixture and the product of the phenol hydroxylation reaction were analyzed by using a high-performance liquid chromatography system (HPLC, Agilent-1100) equipped with an Eclipse XRB-C1899 column (4.6 × 250 mm) using a methanol/H_2O mixture (with a volume ratio of 20/80) as the mobile phase with UV detection at 254 nm.

3. RESULTS AND DISCUSSION

3.1. Influence of the Synthesis Precursor on the Crystallization of Al-Free Mn-β. The chemical composition of the precursor mixture is critical for the hydrothermal synthesis of zeolite β. In order to study the effect of the concentration of each component in the precursor mixture on the crystallization of the Al-free Mn-β, we synthesized a series of Al-free Mn-β samples by independently varying the molar ratio of each component to SiO_2 in the precursor mixture. The XRD results of these Al-free Mn-β samples are listed in Table 1, and the corresponding XRD patterns are shown in Figure S1 in the Supporting Information (SI). These 24 samples belong to four groups (designated as Groups I−IV), which are designed to study the influence of the concentrations of MnO_2, TEA_2O, H_2O, and NaF in the precursor mixture on the crystallization of Al-free Mn-β, respectively. Group I, including samples 1−7, demonstrates that when the molar ratio of $n(MnO_2)$:$n(SiO_2)$ is in the range of 0.005−0.05 zeolite β could form. The amorphous phase(s) forms when the concentration of MnO_2 is too high or too low. Group II, including samples 8−13, indicates that in order to form zeolite β the molar ratio of $n([(TEA)_2O]$:$n(SiO_2)$ in the precursor mixture needs to be larger than 0.20. The positive-charged TEA^+ from TEAOH has a stable tetrahedral structure and good structure-directing function, which could contribute to the formation of the zeolite β.[27] TEA^+ could also balance the negative charge in the framework of zeolite β. Although increasing the concentration of TEAOH in the precursor mixture could significantly facilitate the crystallization of zeolite β, the high cost of TEAOH limits its use. Group III, including samples 14−18, exhibits that the molar ratio of $n(H_2O)$:$n(SiO_2)$ in the precursor mixture should be in the range of 7.5−12.5 in order to obtain pure zeolite β. If the content of H_2O is too low, the precursor mixture is too sticky to be fully stirred, and thus it is hard to form a uniform colloidal solution. However, too much H_2O in the precursor mixture would result in the product consisting of zeolite β and other unidentified phase(s). Group IV, including samples 19−24, suggests that the NaF concentration in the precursor mixture also affects the crystallization of zeolite β. The proper ratio of $n(NaF)$:$n(SiO_2)$ is 0.1−0.3, in which crystalline zeolite β could be synthesized. A too low concentration of NaF would retard the nucleation of the zeolite β crystals, whereas a too high concentration of NaF not only changes the pH of the solution but also decreases the formation rate of the zeolite β nuclei.

In summary, our study shows that for each component in the synthesis precursor there is a concentration range ($n(MnO_2)$/$n(SiO_2)$ = 0.005−0.05, $n([(TEA)_2O]$:$n(SiO_2)$ ≥ 0.2, $n(H_2O)$:$n(SiO_2)$ = 7.5−12.5, and $n(NaF)$:$n(SiO_2)$ = 0.1−0.3), in which crystalline Al-free Mn-β could be obtained. Otherwise, amorphous phase(s) or mixed phases of crystals are produced (see a more detailed discussion in the SI).

3.2. Mn Concentration Analyses and X-ray Diffraction Characterization of Al-Free Mn-β. By increasing the initial molar ratio of MnO_2:SiO_2 in the precursor, it is possible to increase Mn wt % in the synthesized Al-free Mn-β, as shown in Figure 1. The limited amount of active metal (usually under 2 wt %) that can be incorporated into the frameworks currently limits the large-scale applications of the heteroatomic zeolitic materials.[8] However, in our study, Al-free Mn-β with a Mn concentration from 0 to as high as 3.56 wt % could be synthesized. This fact could make our Al-free Mn-β more adaptive to different reactions and therefore expand the range of its potential applications.

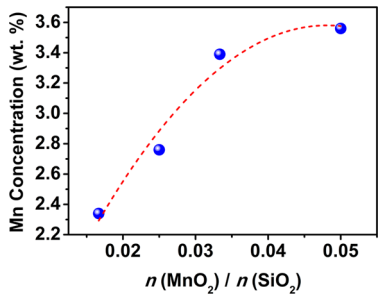

Figure 1. Mn concentration in the Al-free Mn-β as a function of the initial MnO_2:SiO_2 molar ratio in the precursor mixture.

The XRD patterns of the crystalline Al-free Mn-β with different Mn concentrations are similar (as shown in Figure S1 in the SI). A representative pattern of an Al-free Mn-β sample (with 2.34 wt % Mn) synthesized from the precursor mixture of SiO_2:MnO_2:$(TEA)_2O$:H_2O:NaF = 60:1:18:450:10 is shown in Figure 2a, which indicates that the as-synthesized material is well crystallized. This pattern shows six major diffraction peaks at the 2θ angles of 7.7°, 21.5°, 22.6°, 25.4°, 26.8°, and 29.5°, respectively. The last five of these peaks can be assigned to the characteristic diffractions of (300), (302), (304), (008), and (306) planes of polymorph A.[30] This suggests that the synthesized Al-free Mn-β possesses a structure of the β

DOI: 10.1021/am507134g
ACS Appl. Mater. Interfaces 2015, 7, 2424−2432

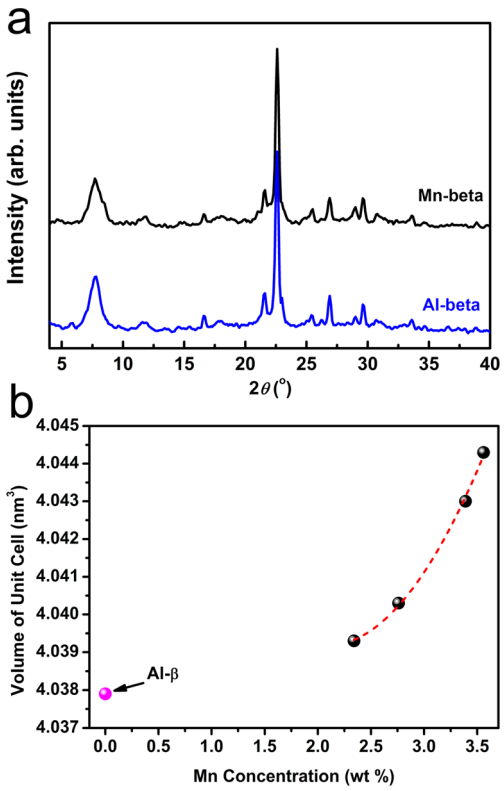

Figure 2. (a) XRD patterns of the synthesized Al-free Mn-β and Al-β zeolite samples. (b) Volume of the unit cell of the synthesized Al-free Mn-β zeolite as a function of Mn concentration in the material (black spheres). The pink sphere represents the volume of the unit cell of the Al-β zeolite.

phase. In addition, compared to the XRD pattern of Al-β (in Figure 2a) or pure silica beta zeolites,[28,29] the peak positions of the Al-free Mn-β slightly shift to lower angles, and there is no extra peak in the XRD pattern of the synthesized Al-free Mn-β. This implies that the Mn is more likely incorporated into the framework of the zeolite rather than existing as the manganese oxides (MnO_x) in the material. The lattice parameters of the Al-free Mn-β zeolite samples with different Mn contents are calculated in the tetragonal system from the five major characteristic diffraction peaks of the polymorph A in their XRD patterns, according to Higgins' report.[30] As the Mn content in the Al-free Mn-β increases, the volume of the unit cell of the material slightly increases (see Figure 2b). This systematic volume change of the unit cell as a function of Mn content also implies the substitution of framework Si atoms with heteroatoms Mn in the β zeolite. The length of the Mn−O bond (0.197 nm) is longer compared to that of the Si−O bond (0.159 nm) or Al−O bond (0.175 nm). Therefore, as Mn isomorphously substitutes Si and/or Al into the framework of the β zeolite, the volume of the unit cell of the β zeolite increases.[25,31]

3.3. Morphology and Surface Studies of Al-Free Mn-β. The morphology of the synthesized crystalline Al-free Mn-β was studied by an FEI Nova Nano 450 SEM at an accelerating voltage of 10 kV. Figure 3 shows a SEM image of the Al-free Mn-β (with 2.76 wt % Mn). This sample consists of irregular-shaped zeolite β particles. The particle size of this Al-free Mn-β zeolite based on this SEM image is approximately in the range of 100−200 nm.

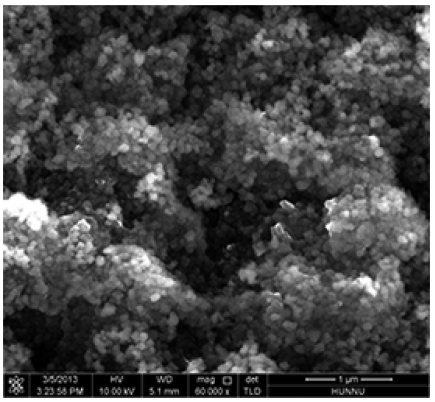

Figure 3. SEM image of Al-free Mn-β zeolite with 2.76 wt % Mn.

Nitrogen adsorption−desorption isotherms of the synthesized Al-free Mn-β (with 2.76 wt % Mn) are measured (see Figure S2 in SI) and show a typical microporous feature of such materials (type-I isotherm). The Brunauer−Emmett−Teller (BET) surface area of the Al-free Mn-β is found to be about 455 m^2/g. This is close to the BET surface area of a pure silica zeolite beta (435 m^2/g) reported by Fong et al.[28] The micropore volume of the Al-free Mn-β determined by the *t-plot* method is about 0.17 cm^3/g, which agrees with the values of micropore volume for pure silica zeolites beta ranging from 0.14 to 0.23 cm^3/g depending on the crystallinity of the materials.[29] Therefore, the results imply that the surface properties of the zeolite beta are not significantly affected by the doped manganese.

3.4. Infrared Spectroscopy of Al-Free Mn-β. The characteristic absorption peaks of β zeolite at about 525 and 575 cm^{-1} have been found in the FT-IR spectrum of the synthesized Al-free Mn-β sample, as shown in Figure 4.[27] The

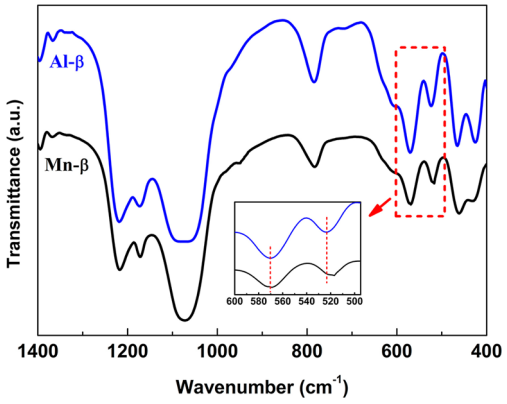

Figure 4. FT-IR spectra of the Al-free Mn-β zeolite with 2.76 wt % Mn and Al-β zeolite. The inset shows an enlarged view of the spectra of the selected area marked by the red rectangular box.

absorption at about 525 cm^{-1} is typically due to the vibration of the framework double four-membered ring (D4R) units, whereas the adsorption at about 575 cm^{-1} could be assigned to the vibration of the five-membered rings in the framework. The absorption bands are well-defined, indicating good crystallinity of the material. The absorption band close to 800 cm^{-1} is due to Si−O−Si symmetric stretching.[22] The FT-IR spectra of the synthesized Al-free Mn-β and Al-β are similar as shown in Figure 4. However, the peaks in the spectrum of Al-free Mn-β shift to lower wavenumbers (i.e., red shift). The two

DOI: 10.1021/am507134g
ACS Appl. Mater. Interfaces 2015, 7, 2424−2432

characteristic peaks for β zeolite shift from 571 to 569 cm^{-1} and from 523 to 518 cm^{-1}, respectively. This could be attributed to the isomorphous substitution of smaller tetrahedrally coordinated Si atoms with larger heteroatoms Mn in the framework, which causes an increase of the average length of the bonds in the D4R and the five-membered ring units in the framework. The FT-IR results further support the statement that Mn substitutes Si into the framework of the zeolite.

3.5. UV−vis Spectroscopy and X-ray Photoelectron Spectroscopy (XPS). The UV−vis diffuse reflectance spectrum of an Al-free Mn-β zeolite sample containing about 2.34 wt % Mn is shown in Figure 5. The Mn-β shows a broad

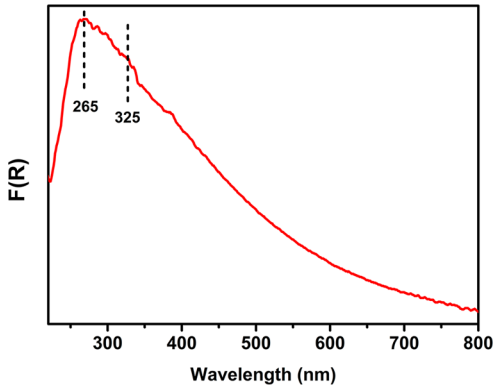

Figure 5. UV−vis DRS spectrum of the Al-free Mn-β sample containing 2.34 wt % Mn.

absorption band in the range of 220−800 nm, peaked at ~265 nm with a weak shoulder at ~325 nm. The absorptions at 265 and 325 nm can be assigned to electron transfer from O^{2-} to the tetrahedrally coordinated Mn^{3+} or/and Mn^{2+} ions in the framework of the zeolite.[22,25,32] According to the literature,[22,25,33] extra-framework Mn species, such as MnO and Mn_3O_4 in channels or on the surface of the zeolite, would cause an absorption band at ~500 nm. However, in our case, although the tail of the broad absorption band extends beyond 500 nm, no obvious absorption band at ~500 nm is observed, which again suggests the Mn is probably doped in the framework of the Al-free Mn-β zeolite. The magnitude of the peak splitting (ΔE) of the Mn 3s peak in the XPS spectra of the as-synthesized Al-free Mn-β samples (see Figure S3 in SI) also indicates that Mn probably exists as Mn^{2+} and/or Mn^{3+} in the as-synthesized Al-free Mn-β. For the Al-free Mn-β after calcination in air, some of the Mn^{2+} species could possibly turn to Mn^{3+} species. This is evidenced by the slightly decreased magnitude of peak splitting of the Mn 3s peak for the calcined samples (see Figure S3b in SI) compared to that of the as-synthesized samples.

3.6. Thermal Analysis of Al-Free Mn-β. The TG/DTA curves of the Al-free Mn-β zeolite (with 2.76 wt % Mn) measured in air are shown in Figure 6. Two distinct regions of weight loss are observed on the TGA curve. The first weight loss of ~2.5% between room temperature and ~200 °C is due to the desorption and removal of water, and the second weight loss of ~18.5% in the temperature range of about 200−650 °C corresponds to the decomposition of the organic template (TEAOH) left in the Al-free Mn-β.[24,34,35] Three exothermic peaks with different intensities are observed on the DTA curve, which is similar to the results reported by Perez-Pariente et al.[27] The first two peaks at 320 and 435 °C are due to the

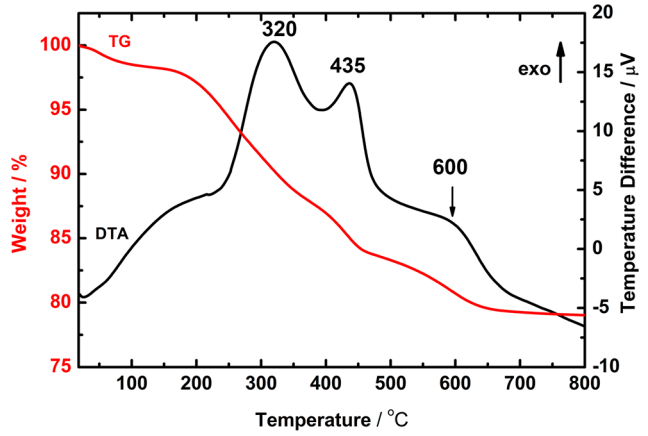

Figure 6. TG and DTA of Al-free Mn-β zeolite with 2.76 wt % Mn.

decomposition of the template species left in the channels of the zeolite. It was previously reported that the decomposition of TEAOH occurred in two steps between 300 and 500 °C due to the different locations of the template species inside the framework of the synthesized zeolite β.[34] The template species oxidized in the second step (at 435 °C) might occupy the sites that are closer to the Brønsted and/or Lewis acid sites (framework manganese sites in our case).[35] The third exothermic peak at about 600 °C probably arises from the further oxidation/combustion of the residue of the template species from the previous oxidation/decomposition steps. In addition, the second exothermic peak of the Al-free Mn-β shifts to a lower temperature compared to that of the Al-β zeolite.[27] This is because the Mn−O bond is longer than both Al−O and Si−O bonds in the framework, which results in a lower density of negative charge around the framework manganese sites. Therefore, the interaction between the TEA^+ cations and the framework of the zeolite becomes weaker as the framework Al/Si is isomorphously substituted by Mn, resulting in a lower temperature of oxidation/decomposition of these template species. Moreover, the TG-DTA curves also show that the synthesized Al-free Mn-β zeolite has a comparable thermal stability as an all-Si β zeolite. This indicates that the substitution of Mn into the framework of the β zeolite does not affect the thermal stability of the β zeolite.

3.7. Catalytic Activity of the Al-Free Mn-β toward the Phenol Hydroxylation Reaction. Under optimized experimental conditions, the synthesized Al-free Mn-β zeolites show remarkable catalytic activity when used as the catalyst in the phenol hydroxylation reaction with H_2O_2 as the oxidant. The systematic studies on the influencing factors to the phenol conversion and product selectivities in the phenol hydroxylation reaction were performed as shown in Table 2. The entries 1−3, 4−7, 8−11, 12−15, and 16−19 are five groups of experiments designed to study the influences of Mn concentration in Al-free Mn-β, m(catalyst)/m(phenol), reaction temperature, reaction time, and n(phenol)/n(H_2O_2) on the conversion and selectivity of the phenol hydroxylation reaction, respectively. Group I, entries 1−3, shows that the phenol conversion increases as the concentration of Mn in the Al-free Mn-β zeolite increases. However, as the concentration of Mn in the catalyst further increases beyond 2.76 wt %, no obvious enhancement of the phenol conversion is observed. This could be due to the detachment of Mn from the framework of the Al-free Mn-β zeolite when the Mn

DOI: 10.1021/am507134g
ACS Appl. Mater. Interfaces 2015, 7, 2424−2432

Table 2. Study on the Catalytic Activity of the Al-Free Mn-β toward the Phenol Hydroxylation Reaction[a]

group	entry	Mn in Al-free Mn-β (wt %)	m(catalyst)/m(phenol)	temperature (°C)	reaction time (hour)	n(phenol)/$n(H_2O_2)$	phenol conversion (% mol)	product selectivity (% mol) CAT[b]	HQ[b]	BQ[b]
Group I: entries 1−3	1	2.34	1/20	80	6	2/1	24.5	60.9	36.1	3.0
	2	2.76	1/20	80	6	2/1	35.2	69.7	27.0	3.3
	3	3.56	1/20	80	6	2/1	35.7	60.3	36.4	3.3
Group II: entries 4−7	4	2.76	1/30	80	6	2/1	19.8	57.2	39.5	3.3
	5	2.76	1/25	80	6	2/1	22.5	60.4	37.1	2.5
	6	2.76	1/20	80	6	2/1	35.3	69.7	26.5	3.8
	7	2.76	1/15	80	6	2/1	35.6	60.5	36.4	3.1
Group III: entries 8−11	8	2.76	1/20	60	6	2/1	17.9	59.8	37.1	3.1
	9	2.76	1/20	70	6	2/1	30.2	62.4	34.7	2.9
	10	2.76	1/20	80	6	2/1	35.2	69.5	28.3	2.2
	11	2.76	1/20	90	6	2/1	36.2	62.3	30.4	7.3
Group IV: entries 12−15	12	2.76	1/20	80	2	2/1	4.2	–	–	–
	13	2.76	1/20	80	4	2/1	25.8	61.9	33.8	4.3
	14	2.76	1/20	80	6	2/1	35.2	69.8	27.1	3.1
	15	2.76	1/20	80	8	2/1	37.2	58.6	34.2	7.2
Group V: entries 16−19	16	2.76	1/20	80	6	4/1	21.4	59.2	36.5	4.3
	17	2.76	1/20	80	6	3/1	27.6	62.3	34.6	3.1
	18	2.76	1/20	80	6	2/1	35.2	69.8	27.3	2.9
	19	2.76	1/20	80	6	1/1	34.5	62.1	34.5	3.4
Group VI: entry 20	20	0 (Al-β)	1/20	80	6	2/1	7.1	54.9	36.2	8.9

[a]This table presents five groups of experiments (that is, entries 1−3, 4−7, 8−11, 12−15, and 16−19, respectively) studying the influences of Mn concentration in Al-free Mn-β, m(catalyst)/m(phenol), reaction temperature, reaction time, and n(phenol)/$n(H_2O_2)$, respectively. For comparison, entry 20 (Group VI) in the table shows the catalytic activity of an Al-β sample toward the phenol hydroxylation reaction. Note that the results of entries 2, 6, 10, 14, and 18 are five parallel trials under exactly the same conditions in order to test the reproducibility of the results. [b]CAT = catechol, HQ = hydroquinone, BQ = p-benzoquinone.

concentration is too high, which causes the decomposition of H_2O_2. Group II, entries 4−7, exhibits that the phenol conversion increases as more catalyst is used in the reaction. However, when the mass ratio of m(catalyst)/m(phenol) reaches 1/20, a further increase of the catalyst could not significantly enhance the phenol conversion. Similar results have been reported for the phenol hydroxylation reaction catalyzed by other catalysts and could be attributed to the thermodynamic and mass transfer limitation at higher reaction rates.[36−39] Group III, entries 8−11, indicates that the phenol conversion increases as the reaction temperature increases. The selectivity for dihydroxybenzenes (including catechol and hydroquinone) in the product first increases when the temperature increases and then significantly decreases when the temperature is above 80 °C, whereas the selectivity for p-benzoquinone in the product is enhanced at the temperature of 90 °C. This could be due to the further oxidation of dihydroxybenzene to p-benzoquinone at temperatures higher than 80 °C. Group IV, entries 12−15, shows that no dihydroxybenzene was produced at the initial 2 h of the reaction. This suggests the reaction has a relatively long induction period. After the initial 2 h, the phenol conversion increases as the reaction proceeds. The selectivity for dihydroxybenzenes in the product reaches a maximum of 96.9% (including 69.8% catechol and 27.1% hydroquinone) at 6 h of the reaction. After 6 h, the color of the solution turns to black due to further oxidation of the produced dihydroxybenzene, which causes a decrease of the selectivity of the dihydroxybenzenes, based on the comparison of results in entries 14 and 15. Group V, entries 16−19, suggests that a relatively higher concentration of H_2O_2 in the reactant solution facilitates the conversion of phenol. However, as the ratio of n(phenol)/$n(H_2O_2)$ decreases from 2/1 to 1/1, both the phenol conversion and dihydroxybenzene selectivity slightly decrease. Considering the cost of the production, n(phenol)/$n(H_2O_2)$ = 2/1 is the most proper in our case of study.

Generally, ∼35.2% phenol conversion and ∼98% dihydroxybenzene selectivity, including 69.7% ± 0.12% catechol and 27.2% ± 0.66% hydroquinone (calculated based on the results of five parallel trials, entries 2, 6, 10, 14, and 18, listed in Table 2), can be obtained using the Al-free Mn-β (with 2.76 wt % Mn) as the catalyst at the optimized experimental conditions (i.e., m(catalyst)/m(phenol) = 1/20, reaction temperature = 80 °C, reaction time = 6 h, and n(phenol)/$n(H_2O_2)$ = 2/1), as shown in Figure 7. The turnover number (TON) of this Al-free Mn-β catalyst for phenol hydroxylation is about 149 at the same conditions. Under the same conditions, the phenol hydroxylation reaction catalyzed by an Al-β catalyst only reaches ∼7.1% phenol conversion and ∼91.1% dihydroxybenzene selectivity (including 54.9% catechol and 36.2% hydroquinone), as shown in entry 20 in Table 2. This indicates that the framework Mn sites are active for phenol hydroxylation.

A possible pathway of the phenol hydroxylation reaction catalyzed by the calcined Al-free Mn-β zeolite is shown in Scheme 1. The mechanism involves the interaction of a metal complex on the framework of the zeolite with H_2O_2, forming OH radicals, which is similar to the previously reported mechanism of phenol hydroxylation catalyzed by other heteroatomic zeolites such as Cu/MCM-41-S, CuNaY, and iron(II)-8-quinolinol/MCM-41.[40−42] Mn ions in the framework of Al-free Mn-β zeolite have unoccupied 3d orbitals and can coordinate with the lone-pair electrons on the O atoms in

DOI: 10.1021/am507134g
ACS Appl. Mater. Interfaces 2015, 7, 2424−2432

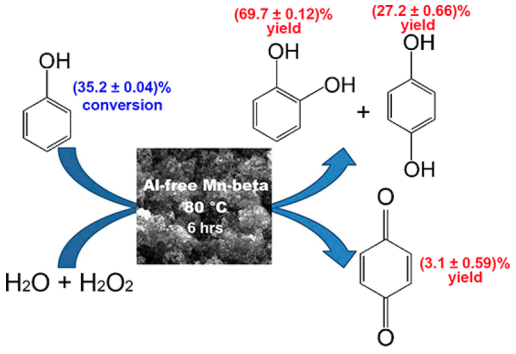

Figure 7. Illustration of the phenol hydroxylation reaction using Al-free Mn-β (with 2.76 wt % Mn) as a catalyst under the optimal experimental conditions. The initial mass ratios of m(phenol):m(catalyst):$m(H_2O_2)$:$m(H_2O)$ are 66:3.3:12:110. The values of phenol conversion and product yields are calculated based on the results of five parallel trials, entries 2, 6, 10, 14, and 18, listed in Table 2.

H_2O_2 molecules. This causes the bonding electrons on the O−O bond to transfer to the coordinated O atom, resulting in the fracture of the O−O bond and the formation of •OH, as shown in step 1 in Scheme 1. The formed •OH, as an electrophile, tends to attack the *ortho* and *para* positions (electrophilic sides) of the aromatic ring of phenol to produce catechol and hydroquinone,[43] as shown in steps 2 and 3 in Scheme 1.

4. CONCLUSIONS

Al-free Mn-β zeolite has been hydrothermally synthesized from precursor mixtures containing $n(SiO_2)$:$n(MnO_2)$:$n[(TEA)_2O]$:$n(H_2O)$:n(NaF) = 60:(0.3−3):(12−18):(450−750):(6−18). The characterization results by XRD, FT-IR, and UV−vis suggest that the synthesized Al-free Mn-β zeolites have a β phase structure with good crystallinity and that Mn isomorphously substitutes Si in the framework of the zeolite. ICP result indicates that the Mn content in the synthesized Al-free Mn-β zeolite can be controlled by varying the concentration of the Mn source in the precursor mixture. The synthesized Al-free Mn-β has a particle size in the range of 100−200 nm. N_2 adsorption−desorption analysis shows that the Al-free Mn-β has a similar BET surface area and microporous volume as the pure silica zeolite β. TG-DTA results show that the Al-free Mn-β zeolite has a thermal stability as good as an all-Si β zeolite. The synthesized Al-free Mn-β zeolites show good catalytic activity toward the phenol hydroxylation reaction. Under the optimized experimental conditions, the turnover number, phenol conversion, and selectivity for dihydroxybenzenes can reach 149, ∼35%, and ∼98%, respectively.

■ ASSOCIATED CONTENT

Supporting Information

Details about the effect of chemical composition of the synthesis precursor to the crystallization of Al-free Mn-β, details about optimizing the experimental conditions in the catalysis tests, XRD and XPS characterizations, and N_2 adsorption−desorption isotherms. This material is available free of charge via the Internet at http://pubs.acs.org.

■ AUTHOR INFORMATION

Corresponding Author

*E-mail: zhenhe@csu.edu.cn.

Notes

The authors declare no competing financial interest.

Scheme 1. Possible Pathway for the Phenol Hydroxylation Reaction Catalyzed by the Synthesized Al-Free Mn-β Zeolite

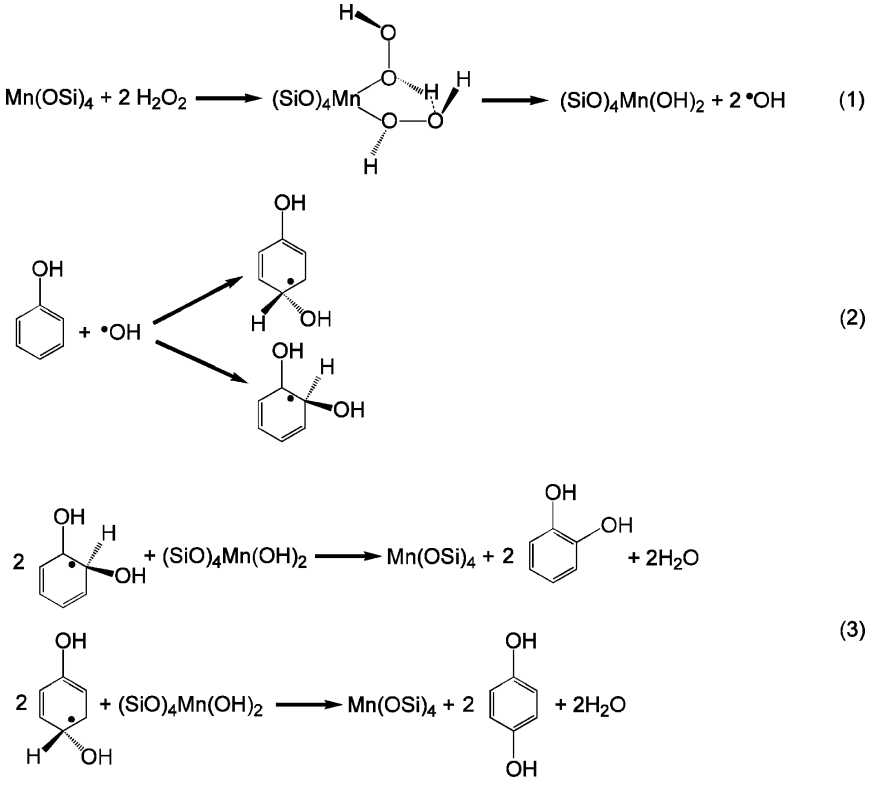

DOI: 10.1021/am507134g
ACS Appl. Mater. Interfaces 2015, 7, 2424−2432

■ ACKNOWLEDGMENTS

This work was supported by the National Natural Science Foundation of China (Grant No. 21303270) and Scientific Research Foundation for the Returned Overseas Chinese Scholars, Ministry of Education of P. R. China (Grant No. 2013[1792]).

■ REFERENCES

(1) Davis, M. E. Ordered Porous Materials for Emerging Applications. *Nature* **2002**, *417*, 813−821.
(2) Corma, A. From Microporous to Mesoporous Molecular Sieve Materials and Their Use in Catalysis. *Chem. Rev.* **1997**, *97*, 2373−2419.
(3) Corma, A. State of the Art and Future Challenges of Zeolites as Catalysts. *J. Catal.* **2003**, *216*, 298−312.
(4) Wadlinger, R. L.; Kerr, G. T.; Rosinski, E. J. A Crystalline Zeolite with Improved Adsorption and Catalytic Properties. US Pat. No 3308069, 1967, Mobil Oil Corporation.
(5) Chen, H.-Y.; Sachtler, W. M. H. Activity and Durability of Fe/ZSM-5 Catalysts for Lean Burn NO_x Reduction in the Presence of Water Vapor. *Catal. Today* **1998**, *42*, 73−83.
(6) Rangus, M.; Mazaj, M.; Arcon, I.; Mali, G.; Kaucic, V. Spectroscopic Investigation of Ti-Modified Aluminum-Free Zeolite-Beta Crystallization. *Chem. Mater.* **2011**, *23*, 1337−1346.
(7) Hould, N. D.; Lobo, R. F. Nanoparticle Precursors and Phase Selectivity in Hydrothermal Synthesis of Zeolite *β*. *Chem. Mater.* **2008**, *20*, 5807−5815.
(8) Hammond, C.; Conrad, S.; Hermans, I. Simple and Scalable Preparation of Highly Active Lewis Acidic Sn-*β*. *Angew. Chem., Int. Ed.* **2012**, *51*, 11736−11739.
(9) Corma, A.; Esteve, P.; Martinez, A.; Valencia, S. Oxidation of Olefins with Hydrogen Peroxide and Tert-Butyl Hydroperoxide on Ti-beta Catalyst. *J. Catal.* **1995**, *152*, 18−24.
(10) Corma, A.; Nemeth, L. T.; Renz, M.; Valencia, S. Sn-zeolite Beta as a Heterogeneous Chemoselective Catalyst for Baeyer-Villiger Oxidations. *Nature* **2001**, *412*, 423−425.
(11) Boronat, M.; Concepcion, P.; Corma, A.; Renz, M. Peculiarities of Sn-Beta and Potential Industrial Applications. *Catal. Today* **2007**, *121*, 39−44.
(12) Corma, A.; Renz, M. Sn-Beta Zeolite as Diastereoselective Water-Resistant Heterogeneous Lewis-Acid Catalyst for Carbon-Carbon Bond Formation in the Intramolecular Carbonyl-Ene Reaction. *Chem. Commun.* **2004**, *5*, 550−551.
(13) Corma, A.; Domine, M. E.; Nemeth, L.; Valencia, S. Al-Free Sn-Beta Zeolite as a Catalyst for the Selective Reduction of Carbonyl Compounds (Meerwein-Ponndorf-Verley Reaction). *J. Am. Chem. Soc.* **2002**, *124*, 3194−3195.
(14) Corma, A.; Domine, M. E.; Valencia, S. Water-resistant Solid Lewis Acid Catalysts: Meerwein-Ponndorf-Verley and Oppenauer Reactions Catalyzed by Tin-Beta Zeolite. *J. Catal.* **2003**, *215*, 294−304.
(15) Izgorodin, A.; Izgorodina, E.; MacFarlane, D. R. Low Overpotential Water Oxidation to Hydrogen Peroxide on a MnO_x Catalyst. *Energy Environ. Sci.* **2012**, *5*, 9496−9501.
(16) Takashima, T.; Hashimoto, K.; Nakamura, R. Inhibition of Charge Disproportionation of MnO_2 Electrocatalysts for Efficient Water Oxidation under Neutral Conditions. *J. Am. Chem. Soc.* **2012**, *134*, 18153−18156.
(17) Gorlin, Y.; Jaramillo, T. F. A Bifunctional Nonprecious Metal Catalyst for Oxygen Reduction and Water Oxidation. *J. Am. Chem. Soc.* **2010**, *132*, 13612−13614.
(18) Cheng, F.; Shen, J.; Peng, B.; Pan, Y.; Tao, Z.; Chen, J. Rapid Room-Temperature Synthesis of Nanocrystalline Spinels as Oxygen Reduction and Evolution Electrocatalysts. *Nat. Chem.* **2011**, *3*, 79−84.
(19) Kim, K. W.; Kim, S. M.; Choi, S.; Kim, J.; Lee, I. S. Electroless Pt Deposition on Mn_3O_4 Nanoparticles via the Galvanic Replacement Process: Electrocatalytic Nanocomposite with Enhanced Performance for Oxygen Reduction Reaction. *ACS Nano* **2012**, *6*, 5122−5129.
(20) Espinal, L.; Suib, S. L.; Rusling, J. F. Electrochemical Catalysis of Styrene Epoxidation with Films of MnO_2 Nanoparticles and H_2O_2. *J. Am. Chem. Soc.* **2004**, *126*, 7676−7682.
(21) Nakayama, M.; Shamoto, M.; Kamimura, A. Surfactant-Induced Electrodeposition of Layered Manganese Oxide with Large Interlayer Space for Catalytic Oxidation of Phenol. *Chem. Mater.* **2010**, *22*, 5887−5894.
(22) Meng, Y.; Genuino, H. C.; Kuo, C.-H.; Huang, H.; Chen, S.-Y.; Zhang, L.; Rossi, A.; Suib, S. L. One-Step Hydrothermal Synthesis of Manganese-containing MFI-Type Zeolite, Mn-ZSM-5, Characterization, and Catalytic Oxidation of Hydrocarbon. *J. Am. Chem. Soc.* **2013**, *135*, 8594−8605.
(23) Raja, R.; Sankar, G.; Thomas, J. M. Powerful Redox Molecular Sieve Catalysts for the Selective Oxidation of Cyclohexane in Air. *J. Am. Chem. Soc.* **1999**, *121*, 11926−11927.
(24) Parida, K. M.; Dash, S. S.; Singha, S. Structural Properties and Catalytic Activity of Mn-MCM-41 Mesoporous Molecular Sieves for Single-Step Amination of Benzene to Aniline. *Appl. Catal., A* **2008**, *351*, 59−67.
(25) Zhang, X.; Liu, P.; Wu, Y.; Yao, Y.; Wang, J. Synthesis and Catalytic Performance of the Framework-Substituted Manganese *β* Zeolite. *Catal. Lett.* **2010**, *137*, 210−215.
(26) Ogura, M.; Okubo, T.; Elangovan, S. P. Hydrocarbon Reformer Trap by Use of Transition Metal Oxide-Incorporated Beta Zeolites. *Catal. Lett.* **2007**, *118*, 72−78.
(27) Perez-Pariente, J.; Martens, J. A.; Jacobs, P. A. Crystallization Mechanism of Zeolite *β* from Bis(tetraethylammonium) Oxide, Sodium Oxide, and Potassium Oxide Containing Aluminosilicate Gels. *Appl. Catal.* **1987**, *31*, 35−64.
(28) Fong, Y. Y.; Bhatia, S. Pure Silica Zeolite Beta Membrane: A Potential Low Dielectric Constant Material for Microprocessor Application. *J. Appl. Sci.* **2007**, *7*, 2040−2045.
(29) Serrano, P.; Van Grieken, R.; Sanchez, P.; Sanz, R.; Rodriguez, L. Crystallization Mechanism of All-Silica Zeolite Beta in Fluoride Medium. *Microporous Mesoporous Mater.* **2001**, *46*, 35−46.
(30) Higgins, J. B.; LaPierre, R. B.; Schlenker, J. L.; Rohrman, A. C.; Wood, J. D.; Kerr, G. T.; Rohrbaugh, W. J. The Framework Topology of Zeolite Beta. *Zeolites* **1988**, *8*, 446−452.
(31) van der Waal, J. C.; Kooyman, P. J.; Jansen, J. C.; van Bekkum, H. Synthesis and Characterization of Aluminum-Free Zeolite Titanium Beta Using Di(cyclohexylmethyl)dimethylammonium as a New and Selective Template. *Microporous Mesoporous Mater.* **1998**, *25*, 43−57.
(32) Velu, S.; Shah, N.; Jyothi, T. M.; Sivasanker, S. Effect of Manganese Substitution on the Physicochemical Properties and Catalytic Toluene Oxidation Activities of Mg-Al Layered Double Hydroxides. *Microporous Mesoporous Mater.* **1999**, *33*, 61−75.
(33) Vetrivel, S.; Pandurangan, A. A Comparative Study on the Catalytic Activity of Mn Containing MCM-41 Molecular Sieves for Oxidation of p-cymene. *Catal. Lett.* **2008**, *120*, 71−81.
(34) Tusar, N. N.; Logar, N. Z.; Arcon, I.; Thibault-Starzyk, F.; Ristic, A.; Rajic, N.; Kaucic, V. Manganese-Containing Silica-Based Microporous Molecular Sieve MnS-1: Synthesis and Characterization. *Chem. Mater.* **2003**, *15*, 4745−4750.
(35) Parker, L. M.; Bibby, D. M.; Patterson, J. E. Thermal Decomposition of ZSM-5 and Silicalite Precursors. *Zeolites* **1984**, *4*, 168−174.
(36) Jin, M.; Yang, R.; Zhao, M.; Li, G.; Hu, C. Application of Fe/Activated Carbon Catalysts in the hydroxylation of Phenol to Dihydroxybenzenes. *Ind. Eng. Chem. Res.* **2014**, *53*, 2932−2939.
(37) Maurya, M. R.; Saklani, H.; Kumar, A.; Chand, S. Dioxovanadium (V) Complexes of Dibasic Tridentate Ligands Encapsulated in Zeolite-Y for the Liquid Phase Catalytic Hydroxylation of Phenol Using H_2O_2 as Oxidant. *Catal. Lett.* **2004**, *93*, 121−127.
(38) Maurya, M. R.; Titinchi, S. J. J.; Chand, S. Liquid-Phase Catalytic Hydroxylation of Phenol Using Cu(II), Ni(II) and Zn(II) Complexes of Aminate Ligand Encapsulated in Zeolite-Y as Catalysts. *Catal. Lett.* **2003**, *89*, 219−227.

DOI: 10.1021/am507134g
ACS Appl. Mater. Interfaces 2015, 7, 2424−2432

(39) Parida, K. M.; Mallick, S. Hydroxylation of Phenol over Molybdovanadophosphoric Acid Modified Zirconia. *J. Mol. Catal. A: Chem.* **2008**, *279*, 104−111.
(40) Zhang, G.; Long, J.; Wang, X.; Zhang, Z.; Dai, W.; Liu, P.; Li, Z.; Wu, L.; Fu, X. Catalytic Role of Cu Sites of Cu/MCM-41 in Phenol Hydroxylation. *Langmuir* **2010**, *26*, 1362−1371.
(41) Wang, J.; Park, J. N.; Jeong, H. C.; Choi, K. S.; Wei, X. Y.; Hong, S. I.; Lee, C. W. Cu^{2+}-Exchanged Zeolites as Catalysts for Phenol Hydroxylation with Hydrogen Peroxide. *Energy Fuels* **2004**, *18*, 470−476.
(42) Liu, C.; Shan, Y.; Yang, X.; Ye, X.; Wu, Y. Iron(II)-8-Quinolinol/MCM-41-Catalyzed Phenol Hydroxylation and Reaction Mechanism. *J. Catal.* **1997**, *168*, 35−41.
(43) Walling, C. Fenton's Reagent Revisited. *Acc. Chem. Res.* **1975**, *8*, 125−131.

DOI: 10.1021/am507134g
ACS Appl. Mater. Interfaces 2015, 7, 2424−2432